Improvement of $Bi_2Sr_2Co_2O_y$ thermoelectric performances by Na doping

G. Çetin Karakaya[1], B. Özçelik[1], O. Nane[2], A. Sotelo[3], Sh. Rasekh[3], M. A. Torres[3], M. A. Madre[3]

[1] Department of Physics, Faculty of Sciences and Letters, Çukurova University, 01330 Adana, (Turkey)
[2]Department of Material Science and Engineering, Faculty of Engineering, Hakkari University, 30000 Hakkari, (Turkey)
[3]Instituto de Ciencia de Materiales de Aragón (CSIC-Universidad de Zaragoza), Mª de Luna, 3. 50018 Zaragoza, (Spain)

Abstract

$Bi_2Sr_{2-x}Na_xCo_2O_y$ thermoelectric materials with x = 0, 0.025, 0.05, 0.075, 0.10, 0.125, and 0.15 have been prepared by solid state reaction. Microstructure has shown an important grain growth when Na is added, leading to very high bulk densities confirmed through density measurements. These modifications have produced a drastic decrease of electrical resistivity without significant modification of Seebeck coefficient. As a consequence, Power Factor has been increased in all Na-doped samples, reaching the maximum value (0.21 $mW/K^2.m$ at 650 ºC) for 0.075 Na samples, which is fairly close to the reported for single crystals.

Keywords: Thermoelectric, Electrical properties, Microstructure, Seebeck coefficient, Cobaltites

Corresponding author: Bekir Özçelik

e-mail: ozcelik@cu.edu.tr

Address: Çukurova University, Faculty of Sciences&Letters, Department of Physics, 01330 Adana, (Turkey)

Tel: +90.322.3386084/2496

Fax: +90.322.3386070

1. Introduction

In the fight against global warming, thermoelectric (TE) materials are very promising due to their ability to directly transforming a thermal gradient into useful electrical energy. In addition, they show very important advantages to harvest wasted heat from many different sources. Moreover, they can also transform solar energy into electricity at lower cost than photovoltaics [1]. As a consequence, the search for materials with high conversion efficiency has been boosted up in the last years. This efficiency is usually quantified through the dimensionless Figure-of-Merit ($ZT = TS^2/\rho\kappa$, where S, ρ, κ, and T, are Seebeck coefficient, electrical resistivity, thermal conductivity and absolute temperature, respectively [2]).

Nowadays, many different semiconducting and intermetallic materials with high performances are used to produce TE modules. On the other hand, many of these materials are composed of heavy and/or toxic elements which can melt or oxidize at high temperatures under air (such as Te, Sb, As, ..) [3]. All these drawbacks, together with their low abundance in earth's crust and high prices, limit the type of applications. In 1997, with the discovery of large Seebeck coefficient and ZT values of 0.26 at 300K in Na_xCoO_2 [4], intensive studies have been performed on new ceramic families with high thermoelectric properties. These works have led to the discovery of different families, as the misfit cobaltites, with promising properties. Their crystal structure is composed of two different layers, with an alternate stacking of a common conductive CdI_2-type CoO_2 layer with a two-dimensional triangular lattice, and a block one, composed of insulating rock-salt-type (RS) layers. Both sublattices (RS block and CdI_2-type CoO_2 layers) possess common *a*- and *c*-axis lattice parameters and β angles but different *b*-axis length, causing a misfit along this direction [5,6]. Some of the most studied cobaltites can be described as $[Ca_2CoO_3]^{RS}[CoO_2]_{1.62}$, and $[Bi_2AE_2O_4]^{RS}[CoO_2]_{b1/b2}$ (where AE: alkaline earth) [7-14], where b_1/b_2 (or b_{RS}/b_{CoO2}) is the misfit factor. In the last family, it is well known that cationic substitution in the rock salt layer using isovalent [15] or aliovalent elements [16,17] can modify the its crystallographic parameters and/or the charge carrier concentration. As a consequence, when adequately performed, it can be applied for tunning up the materials thermoelectric performances.

Taking into account the modification of charge carriers concentration using aliovalent cation doping, in agreement with Koshibae's expression [18], the aim of this study is producing high performances $Bi_2Sr_2Co_2O_y$ sintered materials by substituting Sr^{2+} by Na^+. The structural and microstructural modifications promoted by Na doping will be related with the final thermoelectric properties.

2. Experimental

The initial $Bi_2Sr_{2-x}Na_xCo_2O_y$ polycrystalline ceramics, with x = 0.025, 0.05, 0.075, 0.10, 0.125 and 0.15, were prepared from commercial Bi_2O_3 (Panreac, 98 + %), $SrCO_3$ (98.5 %, Panreac), Na_2CO_3 (Panreac, 98 + %), and Co_2O_3 (Aldrich, 98 + %) powders by the classical solid state route. They were weighed in the appropriate proportions, mixed, and ball milled at 300 rpm for 30 minutes in acetone media. The obtained suspension has been dried under infrared radiation and manually milled to break the agglomerates. The remaining powder was then calcined twice, at 750 and 800 °C for 12 h, with an intermediate milling to decompose the Sr and Na carbonates. The resulting material was uniaxially pressed in form of pellets (~3 x 3 mm^2 section and 15 mm length) at 400 Mpa for 1 minute, and sintered at 810 ºC for 24h with a final furnace cooling [19].
The structural identification of all samples was performed through powder XRD utilizing a Rigaku Miniflex system with Cu Kα radiation (λ = 1.54059 Å) and 2θ between 10 and 70 degrees. Microstructural observations were performed on the samples surface using a Field Emission Scanning Electron Microscope (FESEM, Carl Zeiss Merlin) fitted with energy dispersive spectrometry (EDS) analysis. Moreover, apparent density has been determined in, at least, four samples for each composition and the measurements have been made three times in order to minimize the errors.
Steady-state simultaneous measurements of electrical resistivity and Seebeck coefficient were performed by the standard dc four-probe technique in a LSR-3 apparatus (Linseis GmbH) between 50 and 650 ºC. From these data, Power Factor ($PF= S^2/\rho$) as a function of temperature was calculated to evaluate the samples performances.

3. Results and discussion

Powder XRD patterns for all samples are displayed (from 10 to 40° for clarity) in Fig. 1. As it can be clearly observed, all samples show very similar patterns and most of the peaks (identified with the diffraction planes) correspond to the $Bi_2Sr_{2-x}Na_xCo_2O_y$ phase, in agreement with previously reported data [17,20]. On the other hand, only small amounts of the Co-free $Bi_{0.75}Sr_{0.25}O_{1.375}$ secondary phase [21], can be identified with the peak appearing at about 28 degrees (indicated by *). Moreover, no shift in the thermoelectric phase peaks can be observed, independently of Na content.

The microstructural evolution of samples, as a function of Na content, can be easily observed in Fig. 2, where representative micrographs of their surfaces, are presented. These images show that all samples are formed by two contrasts associated, through EDS, to different phases (numbered in Fig. 2a). Grey contrast (#1) corresponds to the thermoelectric $Bi_2Sr_{2-x}Na_xCo_2O_y$ phase, and white one (#2), to the $Bi_{2.5}SrO_z$ secondary phase, in agreement with XRD data. Moreover, the secondary phase amount is very low in all cases, being nearly unchanged by the Na content. In spite of the negligible effect of Na doping on the secondary phases content, it decreases porosity and leads to larger grain sizes. This fact clearly agrees with previous works in similar ceramic systems, probably due to a liquid phase formation during the sintering process [22,23].

In order to verify this beneficial effect of Na, apparent density has been determined and presented, together with its standard error, in Fig. 3. As it can be seen in the graph, the samples density is raised when increasing Na content, especially for $x > 0.075$. This effect is probably due to their higher amount of liquid phase which raises grain growth rate and decreases porosity. The apparent density values are between 88 and 97 % ρ_{th} (ρ_{th} = 6.15 g/cm^3 [24]).

Fig. 4 displays electrical resistivity variation with temperature, as a function of Na content. The electrical behaviour of samples is clearly modified by Na doping, being semiconducting-like ($d\rho/dT < 0$) for $x < 0.075$, and metallic-like one ($d\rho/dT > 0$) for higher x values. Moreover, the electrical resistivity is decreased until 0.125 Na, slightly increasing for higher Na content. This evolution is in agreement with their higher density, the raise in the charge

carriers concentration, and the larger grain sizes which decreases the number of grain boundaries. As it is well known, Sr^{2+} substitution by Na^{+} in the rock salt layer promotes the oxidation of Co^{3+} to Co^{4+} in the conducting one, leading to higher holes concentration. On the other hand, the raise of electrical resistivity in the 0.15 Na samples is probably due to a higher influence on the charge carrier mobility. In any case, the minimum electrical resistivity values at room temperature (12 mΩ.cm) are lower than the best reported in sintered (around 20 mΩ.cm [25,26]), hot pressed (15 mΩ.cm [6,25]), or laser textured materials (20 mΩ.cm [27]). Moreover, they are fairly close to the ones determined in single crystals (11 mΩ.cm [15]). Furthermore, the minimum values at high temperature (15 mΩ.cm) are still lower than the measured in sintered materials (20-25 mΩ.cm [25,26]), around the obtained in hot pressed materials (16 mΩ.cm [6,25]), and higher than the measured in single crystals (11 mΩ.cm [15]).

Fig. 5 displays the variation of Seebeck coefficient with temperature for all samples. In the figure, it is clear that the Seebeck coefficient is positive in the whole measured temperature range, confirming a conduction mechanism predominantly governed by holes. All the doped samples possess lower Seebeck coefficient than the undoped ones, except in 0.075 Na doped samples, in agreement with the electrical resistivity measurements. The maximum room temperature values are found in the 0 and 0.075 Na samples (120 μV/K), which are in the same order of sintered (105-130 μV/K [25,26]), hot pressed (125 μV/K [6,25]), or laser textured materials (130 μV/K [27]), as well as, single crystals (120 μV/K [15]). On the other hand, at high temperatures, the maximum values are measured in 0.075 Na doped samples (210 μV/K), only comparable to the obtained in sintered materials prepared by solution techniques (210 μV/K [25]). Moreover, they are higher than the measured in sintered (175 μV/K [26]), or hot pressed materials (165 μV/K [6,25]), and single crystals (160 μV/K [15]).

PF variation with temperature is displayed, as a function of Na content, in Fig. 6. In the graph, it can be observed that Na doped samples possess higher PF values than the undoped ones. The maximum PF at room temperature, has been obtained in 0.075, 0.10, and 0.125 Na doped samples (0.08 mW/K^2m). This value is higher than the measured in the undoped samples (0.003 mW/K^2m), laser textured (0.07 mW/K^2m [27]) and sintered materials (0.08-0.06

mW/K^2m [25,26]). On the other hand, they are lower than the reported for hot pressed materials (0.10 mW/K^2m [6,25]), and single crystals (0.13 mW/K^2m [15]). Nevertheless, the raise of PF with temperature in these Na doped samples is higher than the observed in the bibliography, leading to very high PF values (0.21 mW/K^2m at 650 ºC for 0.075 Na samples). This PF is higher than the obtained in sintered (0.12-0.21 mW/K^2m [25,26]) or hot pressed materials (0.16 mW/K^2m [6,25]), and very close to the reported in single crystals (0.23 mW/K^2m [15]).

These results clearly point out to the usefulness of Na doping to enhance grains growth rate and samples density, leading to a drastic decrease of electrical resistivity without significantly modifying Seebeck coefficient. As a consequence, the thermoelectric performances can be improved in a very important manner, approaching their practical applications.

4. Conclusions

In this work, $Bi_2Sr_{2-x}Na_xCo_2O_y$ thermoelectric materials (x = 0, 0.025, 0.05, 0.075, 0.10, 0.125, and 0.15) have been successfully prepared through the classical solid state method. Na doping has promoted an important grain growth and decreased samples porosity. Moreover, densities higher than 85 % of the theoretical one have been reached. The raise in density, together with Na substitution, drastically decreases electrical resistivity without significant modifications of Seebeck coefficient. As a consequence, Na doped samples possess higher PF than the undoped ones. The maximum power factor values have reached 0.21 mW/K^2.m at 650 ºC, which is very close to the reported in the literature for single crystals, clearly indicating that Na doping is a feasible method to produce high performances thermoelectric ceramics.

Acknowledgements

This work is supported by Research Fund of Cukurova University, Adana, Turkey, under grant contracts no: FBA-2016-6626. The Spanish authors thank the Gobierno de Aragón and Fondo Social Europeo (Grupo de Investigacion Consolidado T12) and MINECO-FEDER (MAT2013-46505-C3-1-R) for financial support. Spanish ~~A~~uthors acknowledge the use of Servicio General de Apoyo a la Investigación-SAI, Universidad de Zaragoza.

References

1. W. Liu, X. Yan, G. Chen, Z. Ren, Recent advances in thermoelectric nanocomposites, Nano Energy 1 (2012) 42-56.

2. D.M. Rowe, in: D.M. Rowe (Ed.), Thermoelectrics Handbook: Macro to Nano, 1st edn, CRC Press, Boca Raton, FL, 2006, pp. 1-3–1-7.

3. J. Ander Santamaria, J. Alkorta, J. Gil Sevillano, Microcompression tests of single-crystalline and ultrafine grain Bi_2Te_3 thermoelectric material, J. Mater. Res. 30 (2015) 2593-2604.

4. I. Terasaki, Y. Sasago, K. Uchinokura, Large thermoelectric power in $NaCo_2O_4$ single crystals, Phys. Rev. B 56 (1997) 12685–12687.

5. A. Maignan, S. Hebert, M. Hervieu, C. Michel, D. Pelloquin, D. Khomskii, Magnetoresistance and magnetothermopower properties of Bi/Ca/Co/O and Bi(Pb)/Ca/Co/O misfit layer cobaltites, J. Phys.: Condens. Matter 15 (17) (2003) 2711–2723.

6. H. Itahara, C. Xia, J. Sugiyama, T. Tani, Fabrication of textured thermoelectric layered cobaltites with various rock salt-type layers by using *b*-$Co(OH)_2$ platelets as reactive templates, J. Mater. Chem. 14 (1) (2004) 61–66.

7. M. A. Madre, F. M. Costa, N. M. Ferreira, A. Sotelo, M. A. Torres, G. Constantinescu, Sh. Rasekh, J. C. Diez, Preparation of high-performance $Ca_3Co_4O_9$ thermoelectric ceramics produced by a new two-step method, J. Eur. Ceram. Soc. 33 (2013) 1747-1754.

8. A. C. Masset, C. Michel, A. Maignan, M. Hervieu, O. Toulemonde, F. Studer, B. Raveau, J. Hejtmanek, Misfit-layered cobaltite with an anisotropic giant magnetoresistance: $Ca_3Co_4O_9$, Phys. Rev. B 62 (1) (2000) 166–175.

9. A. Sotelo, Sh. Rasekh, M. A. Madre, E. Guilmeau, S. Marinel, J. C. Diez, Solution-based synthesis routes to thermoelectric $Bi_2Ca_2Co_{1.7}O_x$, J. Eur. Ceram. Soc. 31 (2011) 1763-1769.

10. A. Maignan, D. Pelloquin, S. Hebert, Y. Klein, M. Hervieu, Thermoelectric power in misfit cobaltites ceramics: optimization by chemical substitutions, Bol. Soc. Esp. Ceram. V. 45 (3) (2006) 122–125.

11. K. Rubesova, T. Hlasek, V. Jakes, S. Huber, J. Hejtmanek, D. Sedmidubsky, Effect of a powder compaction process on the thermoelectric properties of $Bi_2Sr_2Co_{1.8}O_x$ ceramics, J. Eur. Ceram. Soc. 35 (2015) 525–531.

12. A. Sotelo, M. A. Torres, G. Constantinescu, Sh. Rasekh, J. C. Diez, M. A. Madre, Effect of Ag addition on the mechanical and thermoelectric performances of annealed $Bi_2Sr_2Co_{1.8}O_x$ textured ceramics, J. Eur. Ceram. Soc. 32 (2012) 3745-3751.

13. W. Kobayashi, S. Hebert, H. Muguerra, D. Grebille, D. Pelloquin, A. Maignan, Thermoelectric properties in the misfit-layered-cobalt oxides $[Bi_2A_2O_4][CoO_2]_{b1/b2}$ (A=Ca, Sr, Ba, b(1)/b(2)=1.65, 1.82, 1.98) single crystals. In I. Kim (Ed.), Proceedings ICT 07: Twenty-sixth international conference on thermoelectrics, Korea. 2008. pp. 117-120.

14. G. Constantinescu, Sh. Rasekh, M. A. Torres, M. A. Madre, J. C. Diez, A. Sotelo, Enhancement of the high-temperature thermoelectric performance of $Bi_2Ba_2Co_2O_x$ ceramics, Scr. Mater. 68 (2013) 75-78.

15. N. Sun, S. T. Dong, B. B. Zhang, Y. B. Chen, J. Zhou, S. T. Zhang, Z. B. Gu, S. H. Yao, Y. F. Chen, Intrinsically modified thermoelectric performance of alkaline-earth isovalently substituted $[Bi_2AE_2O_4][CoO_2]_y$ single crystals, J. Appl. Phys. 114 (2013) 043705.

16. W. Shin, N. Murayama, Thermoelectric properties of (Bi,Pb)-Sr-Co-O oxide, J. Mater. Res. 15 (2) (2000) 382-386.

17. A. Sotelo, Sh. Rasekh, E. Guilmeau, M. A. Madre, M. A. Torres, S. Marinel, J. C. Diez, Improved thermoelectric properties in directionally grown $Bi_2Sr_2Co_{1.8}O_y$ ceramics by Pb for Bi substitution, Mater. Res. Bull. 46 (2011) 2537-2542.

18. W. Koshibae, K. Tsutsui, S. Maekawa, Thermopower in cobalt oxides, Phys. Rev. B 62 (2000) 6869-6872.

19. M. A. Madre, Sh. Rasekh, J. C. Diez, A. Sotelo, New solution method to produce high performance thermoelectric ceramics: A case study of Bi-Sr-Co-O, Mater. Lett. 64 (2010) 2566-2568.

20. M. Kato, Y. Goto, K. Umehara, K. Hirota, I. Terasaki, Synthesis and physical properties of Bi-Sr-Co-oxides with 2D-triangular Co layers intercalated by iodine, Phys. B 378-380 (2006) 1062-1063.

21. D. Mercurio, J. C. Champarnaud-Mesjard, B. Frit, P. Conflant, J. C. Boivin, T. Vogt, Thermal evolution of the crystal-structure of the rhombohedral $Bi_{0.75}Sr_{0.25}O_{1.375}$ phase - A single-crystal neutron-diffraction study, J. Solid State Chem. 112 (1994) 1-8.

22. B. Ozkurt, Improvement of the critical current density in Bi-2223 ceramics by sodium–silver co-doping, J. Mater. Sci.: Mater. Electron. 25 (2014) 3295-3300.

23. M. Gursul, A. Ekicibil, B. Ozçelik , M. A. Madre, A. Sotelo, Sintering Effects in Na-Substituted Bi-(2212) Superconductor Prepared by a Polymer Method, J. Supercond. Nov. Magn. 28 (2015) 1913-1924.

24. Q. L. He, Z. Qin, J. Zhang, F. Gao, X. Hu, H. Z. Song, Enhanced Thermoelectric Properties of Hole-Doped $Bi_{2-x}Ba_xSr_2Co_2O_y$ Ceramics, J. Electron. Mater. 43 (2014) 1432-1435.

25. M. A. Torres, A. Sotelo, Sh. Rasekh, I. Serrano, G. Constantinescu, M. A. Madre, J. C. Diez, Improvement of thermoelectric properties of $Bi_2Sr_2Co_{1.8}O_x$ through solution synthetic methods, Bol. Soc. Esp. Ceram. V. 51 (2012) 1-6.

26. E. Combe, R. Funahashi, F. Azough, R. Freer, Relationship between microstructure and thermoelectric properties of $Bi_2Sr_2Co_2O_x$ bulk materials, J. Mater. Res. 29 (2014) 1376-1382.

27. J. C. Diez, Sh. Rasekh, M. A. Madre, E. Guilmeau, S. Marinel, A. Sotelo, Improved Thermoelectric Properties of Bi-M-Co-O (M = Sr, Ca) Misfit Compounds by Laser Directional Solidification, J. Electron. Mater. 39 (2010) 1601-1605.

Figure captions

Figure 1. Powder XRD diagrams for the $Bi_2Sr_{2-x}Na_xCo_2O_y$ sintered samples for x = 0 (a); 0.025 (b), 0.05 (c); 0.075 (d); 0.10 (e); 0.125 (f); and 0.15 (g). Crystallographic planes have been indicated on the peaks corresponding to the thermoelectric phase. * indicates the peak corresponding to the Co-free $Bi_{0.75}Sr_{0.25}O_{1.375}$ secondary phase.

Figure 2. SEM micrographs of surfaces from representative $Bi_2Sr_{2-x}Na_xCo_2O_y$ samples with x = 0 (a); 0.05 (b); 0.10 (c); and 0.15 (d). The different phases are indicated by arrows, 1) $Bi_2Sr_{2-x}Na_xCo_{1.8}O_y$; and 2) $Bi_{2.5}SrO_z$.

Figure 3. Apparent density of $Bi_2Sr_{2-x}Na_xCo_2O_y$ samples, together with their standard error, as a function of Na content.

Figure 4. Temperature dependence of electrical resistivity for $Bi_2Sr_{2-x}Na_xCo_2O_y$ samples with x = 0 (▲); 0.025 (▼); 0.05 (◆); 0.075 (◣); 0.10 (●); 0.125 (◢); and 0.15 (■).

Figure 5. Temperature dependence of the Seebeck coefficient for $Bi_2Sr_{2-x}Na_xCo_2O_y$ samples with x = 0 (▲); 0.025 (▼); 0.05 (◆); 0.075 (◣); 0.10 (●); 0.125 (◢); and 0.15 (■).

Figure 6. Temperature dependence of the power factor for $Bi_2Sr_{2-x}Na_xCo_2O_y$ samples with x = 0 (▲); 0.025 (▼); 0.05 (◆); 0.075 (◣); 0.10 (●); 0.125 (◢); and 0.15 (■).

Figure 1

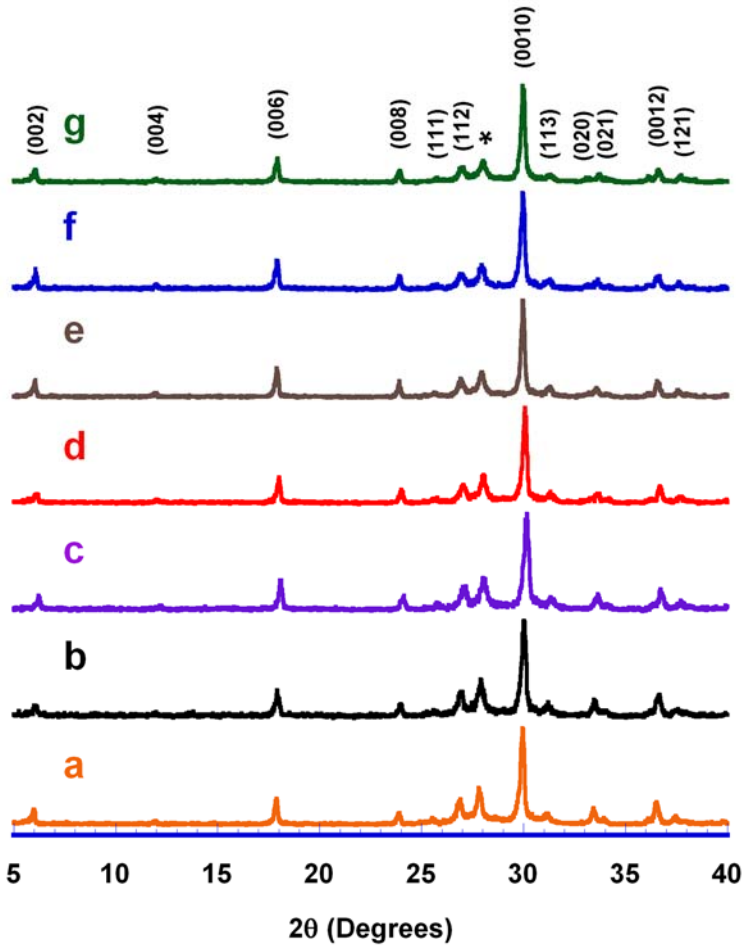
(0010)
(002)
g
(004)
(006)
(008)
(111)
(112)
*
(113)
(020)
(021)
(0012)
(121)
f
e
d
c
b
a
5
10
15
20
25
30
35
40
2θ (Degrees)

Figure 2

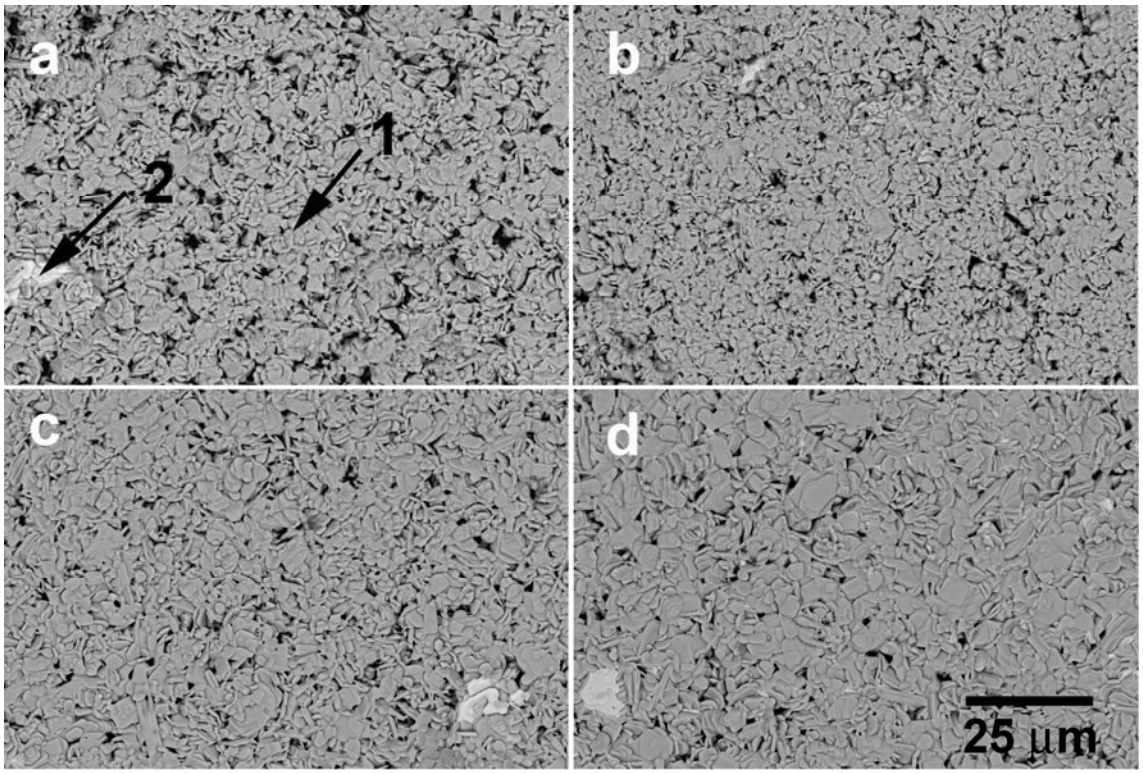

Figure 3

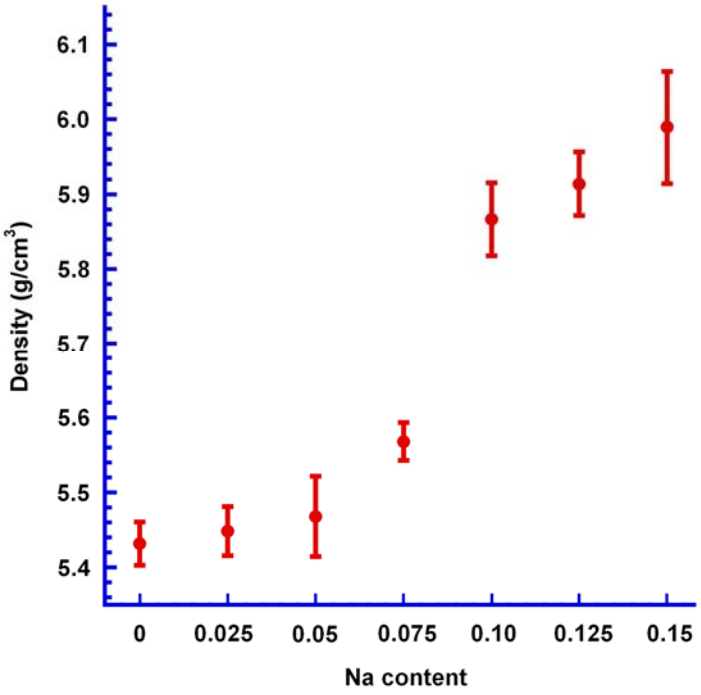
Density (g/cm^3)
6.1
6.0
5.9
5.8
5.7
5.6
5.5
5.4
0
0.025
0.05
0.075
0.10
0.125
0.15
Na content

Figure 4

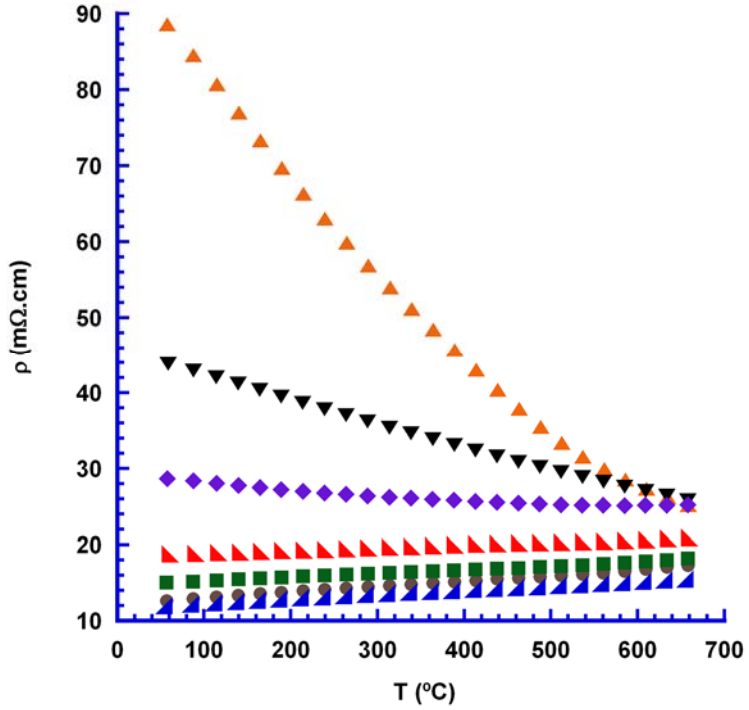

Figure 5

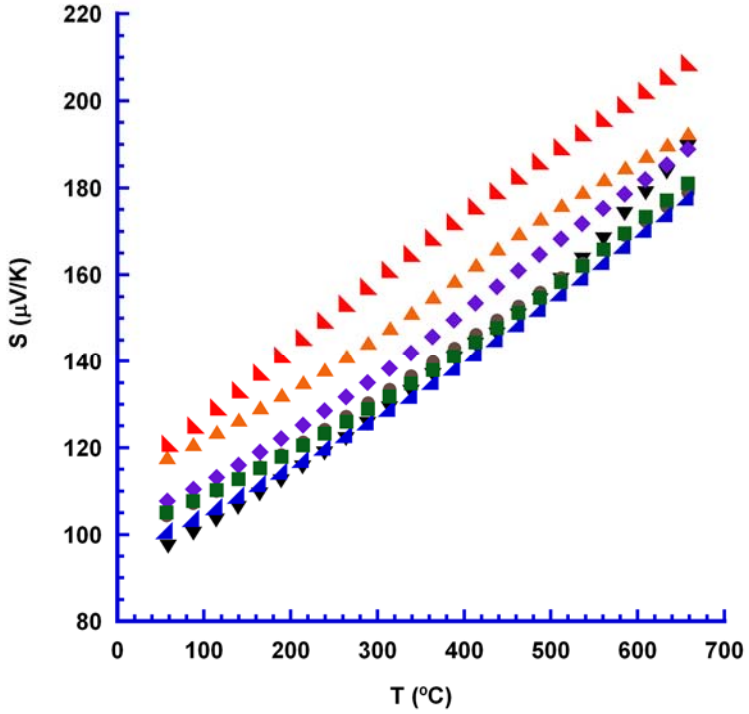
220
200
180
160
140
120
100
80
S (μV/K)
0
100
200
300
400
500
600
700
T (°C)

Figure 6